AGU PUBLICATIONS

JGR

Journal of Geophysical Research: Space Physics

RESEARCH ARTICLE

10.1002/2015JA021322

Key Points:

- Perturbation zonal velocity
- Impact of varying zonal velocity of the perturbations
- L band scintillation forecast

Correspondence to:
M. S. Bagiya,
bagiyamala@gmail.com

Citation:
Bagiya, M. S., R. Sridharan, S. Sunda, L. Jose, T. K. Pant, and R. Choudhary (2015), Impact of the perturbation zonal velocity variation on the spatio/temporal occurrence pattern of L band scintillation—A case study, *J. Geophys. Res. Space Physics*, *120*, 5882–5889, doi:10.1002/2015JA021322.

Received 14 APR 2015
Accepted 21 JUN 2015
Accepted article online 24 JUN 2015
Published online 14 JUL 2015

Impact of the perturbation zonal velocity variation on the spatio/temporal occurrence pattern of L band scintillation—A case study

Mala S. Bagiya[1], R. Sridharan[2], Surendra Sunda[3,4], Lijo Jose[2,5], Tarun K Pant[6], and Rajkumar Choudhary[6]

[1]Indian Institute of Geomagnetism, Navi Mumbai, India, [2]Physical Research Laboratory, Ahmedabad, India, [3]Space Application Centre, Ahmedabad, India, [4]On deputation from Airport Authority of India, [5]St. Berchman's College, Changanasserry, India, [6]Space Physics Laboratory, Trivandrum, India

Abstract The earlier evolved method for the forecast of the spatiotemporal variation of L band scintillation based on the expected variation of the perturbations, under favorable ionospheric/thermospheric conditions, has been refined by duly accounting for the local time variation of the zonal velocity of the perturbations. The unique combination of the two geostationary satellites (GSAT-8 and GSAT-10) over the Indian zone has been used to estimate the typical local time dependence of the perturbation velocities by closely following identifiable features in the scintillation pattern. The measured velocities, that registered a steady decrease with the progression of night, had been shown to significantly alter the forecast pattern of the scintillations with respect to longitude and local time. The significant improvement in the forecast pattern has been demonstrated through a case study putting the forecast method on a firmer footing.

1. Introduction

During postsunset hours, very often, the equatorial and low-latitude ionosphere behaves chaotically, by allowing the generation of multispectral plasma density irregularities, a phenomenon well known as equatorial spread *F* (ESF). The irregularity spectrum contains scale sizes of several orders of magnitude ranging from hundreds of kilometer to tens of centimeter. The different scale sizes have different manifestations like intensity depletions in thermospheric airglow images, density depletions in satellite and rocket in situ measurements, phase and amplitude scintillations of satellite to ground (VHF and UHF) signals, upward moving plasma plumes in VHF coherent backscatter radar maps, and spread in the *F* region reflected echoes as seen in ionograms. Among all these manifestations, the phase and amplitude scintillations of satellite to ground signals have significant practical importance. The ESF density irregularities dilute the accuracy of the satellite-based positioning by introducing extra delays as the signals traverse from satellite to ground. During the presence of strong ESF irregularities/scintillations, the ground receiver may even lose its lock, or in other words, lose synchronization of the satellite signals, making it unusable for estimating the receiver position. In order to get precise satellite-based positioning and navigation, detailed study of ESF irregularities is mandatory. As mentioned above, since the ESF is a multidimensional phenomenon, getting a handle on its initiation, its dynamics including its evolution, assessment of its duration during the course of a given night, and bringing all these to a level of forecast are very essential so that necessary warnings could be given in advance to the potential users.

The two important aspects responsible for the generation of ESF plasma density irregularities are (i) favorable background ionospheric-thermospheric conditions and (ii) the plasma density perturbations at the base of the *F* region that initiate the instability. After local sunset, in the absence of production of ionization, the equatorial *F* region typically moves upward due to the prereversal enhancement of the eastward zonal electric field before it turns westward, and the bottomside *F* region electron densities steadily decay due to recombination. Both the above processes ultimately raise the *F* region base to higher altitudes, and the resultant situation, which is analogous to the heavier fluid being supported by a lighter fluid, is highly unstable. On such occasions, electron density perturbations, if any, at the base height of *F* region could initiate the Rayleigh-Taylor instability which would in turn allow the perturbation to grow in amplitude extending in height.

During their evolution, the irregularities are known to move eastward since their root cause, namely, the perturbations, move eastward with finite velocities. The velocity of the density perturbations had been shown to vary anywhere between 150 and 300 m/s for midlatitudes, falling very much under the category of gravity waves [*Oliver et al*., 1997] which are generally believed to be responsible for the perturbation in the ionospheric plasma. Earlier, attempts had been made to estimate the irregularity zonal drifts either by spaced receiver technique or by using radar interferometry during ESF conditions [e.g., *Chandra et al*., 1970; *Rastogi et al*., 1972; *Basu et al*., 1980; *Kudeki et al*., 1981; *Fejer et al*., 1985; *Bhattacharyya et al*., 2001]. Using spaced receiver technique, *Misra* [1973] had compared the apparent drifts of ground diffraction pattern on spread *F* and nonspread *F* nights over the Indian equatorial station Thumba and reported that on spread *F* days the apparent drift was 1.5 times higher than that of the nonspread *F* days, with the difference being prominent during premidnight hours. *Fejer et al*. [1985] had compared the background plasma drift using the Jicamarca radar with that of the irregularity drift from spaced receiver method measured at Ancon, Peru, and had highlighted the differences. On the other hand, using long-term Jicamarca radar observations, climatological studies including seasonal, solar cycle, and geomagnetically disturbed time, behavior of both the *F* region zonal and vertical plasma drift variations have been carried out by *Fejer et al*. [1991, 2005]. *Abdu et al*. [1985] had studied extensively the irregularity zonal drifts from Brazilian low latitudes using spaced VHF polarimeter measurements. They had stated that, in the presence of weak vertical electric field [*Ossakow and Chaturvedi*, 1978; *Tsunoda*, 1981], the measured irregularity zonal drift could be comparable to the background plasma drift. They had also ruled out any contribution of vertical velocity in their measurements. However, the reported drift values were significantly higher than the background zonal velocity measured by the Jicamarca radar at ~300–400 km altitude, and this has been attributed to the possible latitudinal variation and the vertical shears in the equatorial *F* region.

Quite a few studies have been performed from ground as well as space to estimate the irregularity zonal drift using either plasma bubbles or scintillation patches as tracers [e.g., *Kil et al*., 2002; *de Paula et al*., 2002; *Martinis et al*., 2003; *Immel et al*., 2004; *England and Immel*, 2012; *Nade et al*., 2013]. More recently, the spaced GPS receiver technique has been extensively used to study the dynamics of the ionospheric irregularities [e.g., *Kil et al*., 2000, 2002; *Ledvina et al*., 2004; *Otsuka et al*., 2006; *Muella et al*., 2009]. *de Paula et al*. [2002] had carried out a detailed analysis using two ground-based GPS receivers over South American sector and had shown that the eastward velocity of the irregularity could range from 160 ms^{-1} to 100 ms^{-1} with a tendency to decrease beyond midnight. Their method however suffered a limitation due to the finite satellite movement during the time of observation. In spite of this limitation, the apparent velocity can still be calculated and can be approximated to the true velocity [*Kil et al*., 2000, 2002; *de Paula et al*., 2002].

1.1. Justification

In the present paper, a simpler and more straightforward method, without any of the limitations of the spaced GPS receiver technique, has been evolved on the basis of observations from geostationary satellites. The ultimate aim, however, is to measure the irregularity zonal drift and its temporal variation, if any, all through the night, on which new statistics on nighttime *F* region zonal plasma drift during different seasons and solar activity/geophysical conditions could eventually be built. It has already been demonstrated that the occurrence pattern of the scintillation patches are closely tied up to the perturbations in the base of the *F* region [*Bagiya and Sridharan*, 2011; *Sridharan et al*., 2014] and therefore the zonal movement of the irregularities would directly correspond to the zonal velocity of the perturbations themselves. As a first step, the preliminary results obtained from a recent campaign conducted over the Indian equatorial latitudes are presented and the consequences in the formulation of spatiotemporal maps of scintillations are discussed. If the irregularity zonal drifts are known, along with its temporal variation over a given location, then the estimated time of its arrival over the adjacent longitudes can be determined precisely and more accurate warnings could be issued on the impending scintillations.

In the recent times, systematic attempts to forecast well in advance, (i) the occurrence of L band scintillation over equatorial and low latitudes, (ii) its duration, (iii) strength, and (iv) its latitudinal extent have been made with reasonable success [*Bagiya and Sridharan*, 2011; *Sridharan et al*., 2012; *Bagiya et al*., 2013]. *Sridharan et al*. [2012] had developed a novel method to forecast the occurrence timing and possible duration of the L band scintillation using GPS total electron content (TEC) over the equator as the base data. In spite of their oversimplifying assumptions that the fundamental frequency components of the perturbation retain their relative amplitudes and phases throughout day and night and the complexities associated with the continuously moving GPS satellite platforms, their forecasts on the occurrence of L band scintillations were fairly successful. After making a reasonable forecast for the temporal evolution of L band scintillation over a given location, Trivandrum (8.5°N, 76.91°E; dip latitude 0.5°N), *Sridharan et al*. [2014] attempted to make the spatiotemporal forecast of the occurrence pattern over the Indian region. These maps were generated following the improved method given by *Bagiya et al*. [2014]. In this method, instead of the GPS-TEC, the $[f_oF_2]^2$ data, which are proportional to the *F* region electron density maximum, obtained from an ionosonde at Trivandrum, had been made use of in generating the synthetic perturbations that are likely to be present during the night. More details have been provided in *Sridharan et al*. [2014]. With the basic knowledge that the perturbations move eastward with a finite velocity "*v*," it could be surmised that the train of gravity wave perturbations over any location must have traversed from west of this location with this velocity. Once the perturbations retain their characteristic features, it would imply that any particular feature that passes over Trivandrum would have crossed over another location west of Trivandrum at an earlier time, dictated only by the zonal velocity *v*. The typical zonal velocity, estimated during the observation period by using the nearby GPS passes and the GSAT data, turned out to be ~80 ms^{-1}. In their analysis, *Sridharan et al*. [2014] had taken this value as a representative velocity for the whole of the night. Although the spatiotemporal maps could be generated successfully to a reasonable extent, there were still some discrepancies, when compared with actual observations of scintillations. Few scintillation patches were seen to occur where they were not expected as per the forecast maps generated by *Sridharan et al*. [2014]. The possible variation in the zonal velocity of the perturbation during the course of the night due to certain external forcings was indicated as one of the possible causes for such deviations. This calls for a systematic study of the impact of the zonal velocity variation of the perturbation on the spatiotemporal occurrence pattern of the scintillations. To avoid the limitations imposed due to the finite movement of the GPS satellites in the zonal velocity estimates and to account for the zonal velocity variations while making the spatiotemporal forecast of L band scintillations, a couple of dedicated campaigns were conducted during April 2012 and April 2013 from Trivandrum. The recently launched Indian geostationary satellites GSAT-8 and GSAT-10 beacons (for more details, please refer to *Bagiya et al*. [2014]) were made use of in the study. The following sections describe the simple method for the estimation of velocities along with its application/impact in the spatiotemporal forecast of L band scintillations.

2. Observations and Methodology

Ideally, a realistic estimation of the zonal velocity of the perturbation/irregularities requires at least two stationary ionopsheric piercing points (IPPs) located close by but distinctly separated. If the IPPs moved as in the case of GPS satellite reception, then the estimated velocity may not be a true representation but could only be construed as apparent velocity [*Kil et al*., 2000, 2002; *de Paula et al*., 2002]. The observation of the Indian geostationary satellite signals from two closely spaced ground receivers provided the right opportunity to estimate the desired zonal perturbation/irregularity drift. As the irregularity patches are magnetic field aligned, and as the magnetic equator over India is nearly parallel to the geographic equator, two zonally separated receivers near the equator but not necessarily in the same latitude would also serve our purpose. The longitudinal difference of the two stationary IPPs from ground will correspond to the zonal distance between them. The observed zonal distance along with the time difference between two nearby observable scintillation patches/features will yield the east-west component of the irregularity drift velocity.

The L1 band transmission from the two Indian geostationary satellites at 55°E (GSAT-8: PRN 127) and at 82.98°E (GSAT-10: PRN 128) launched as part of the Indian satellite-based augmentation system, GAGAN (GPS Aided Geo Augmented Navigation), had been used in the present study. Figure 1 shows schematically the experimental setup during the campaign period of April 2013. Two Satellite-Based Augmentation System (SBAS)-enabled GPS receivers were operated, one from Trivandrum (8.5°N, 76.9°E; 0.5°S geomagnetic) and the other from Equatorial Geophysical Research Laboratory, Tirunelveli (8.7°N, 77.8°E; 0.13°N geomagnetic), during 15 April to 22 April 2013, as a part of the campaign. Table 1 gives the look angles for the two geostationary satellites from the two ground stations. The receiver at Trivandrum is part of the

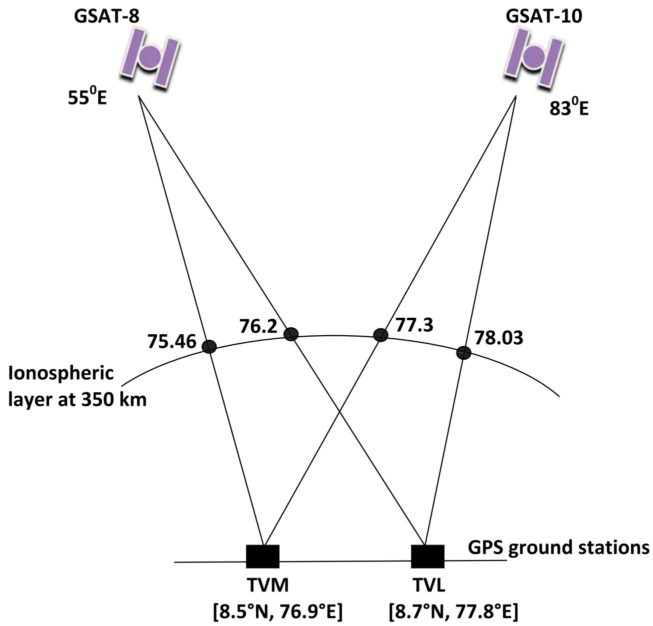

Figure 1. Schematic showing the experimental setup during the campaign period of April 2013. Two SBAS-enabled GPS receivers, one operated from Trivandrum (8.5°N, 76.9°E; 0.5°N geomagnetic) and the other from Equatorial Geophysical Research Laboratory, Tirunelveli (8.7°N, 77.8°E; 0.13°N geomagnetic), are shown along with the IPP longitudes for two GEO satellites GSAT-8 and GSAT-10 over the respective receivers. (Note: Figure is not to the scale).

GAGAN network, while the one operated from Tirunelveli was set up by the Space Physics Laboratory, Trivandrum. Although the actual campaign period was planned from 11 April to 26 April 2013, due to logistics and other practical problems, both the receivers could be operated only for 8 days, and on the remaining days only the receiver at Trivandrum was operational. Although both the receivers were capable of receiving the signals at L1 (1.575 MHz) and L5 (1.176 MHz) frequencies, only the L1 data that contain the coded navigation signals were used in the present study. The L5 generally contains the clock and ephemeris information pertaining to that particular PRN. The IPP corresponding to GSAT-8 is at 75.46°E for Trivandrum and at 76.15°E for Tirunelveli, while for GSAT-10 they are at 77.29°E and 78.03°E, respectively (Figure 1).

The L1 scintillation from PRN 128 are extracted and examined here. The ground receivers recorded the signal intensity at the rate of 50 Hz. The scintillation index (S_4) is calculated by the receiver using the 3000 data points collected over 60 s. The S_4 index is defined as the normalized standard deviation of the received signal power intensity [*Yeh and Liu*, 1982] expressed as

$$S_4 = \sqrt{\frac{\langle SI^2 \rangle - \langle SI \rangle^2}{\langle SI \rangle^2}}$$

Here SI is the signal intensity. The IPP longitude separation between Trivandrum and Tirunelveli for PRN 128 is ~0.74° corresponding to a zonal distance of ~81.29 km. The time taken by the distinct but identical scintillation patches to travel this distance is used to calculate the zonal drift velocity at different times during the night.

3. Zonal Velocity Estimates and Its Nocturnal Variation

The ESF irregularities were observed on all the eight nights of simultaneous observations from Trivandrum and Tirunelveli. On 21 April, the ESF was rather weak as seen in the scintillation index and therefore not considered in the present exercise. The temporal variations of S_4 index during 19:00 LT to 03:00 LT (27:00 h) on 2 days of 15 April and 16 April are reproduced in Figure 2. The continuous line shows PRN 128 observations from Trivandrum, while the dotted line represents the same from Tirunelveli. The clear time lag in the evolution of the scintillation patches at Trivandrum and Tirunelveli could be noticed. On 15 April, four distinct scintillation patches appeared between 21:00 LT and 01:00 LT (25:00 h) (Figure 2a). On this day, the velocities could be estimated at least at four points shown by upward pointing arrows. The increasing distance between the pair of arrows indicates the tendency

Table 1. Azimuth and Elevation Angles for GSAT-8 and GSAT-10 From the Two Ground Stations

	GSAT-8		GSAT-10	
Station	Azimuth	Elevation	Azimuth	Elevation
Trivandrum	250°	62.6°	144°	77.8°
Tirunelveli	250°	61.6°	149°	78.1°

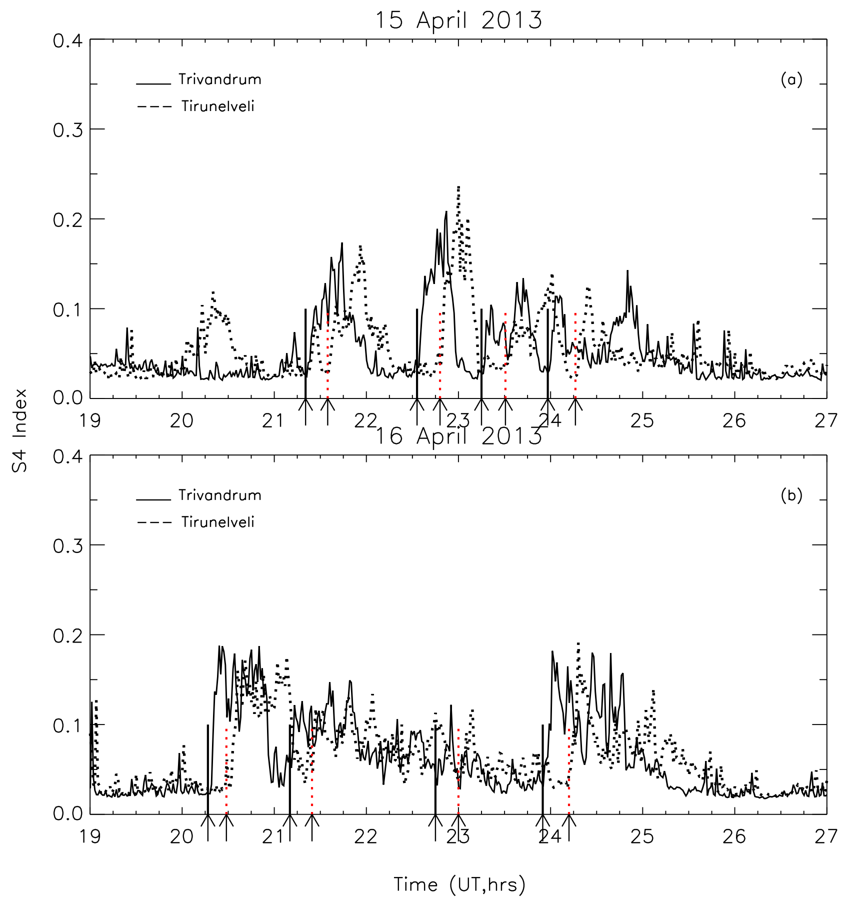

Figure 2. (a) Temporal variation of S_4 index as observed by GSAT-10 over Trivandrum (8.5°N, 76.9°E; solid lines) and Tirunelveli (8.7°N, 77.8°E; dotted line) during 19:00 LT to 03:00 LT (27:00 h) on 15 April 2013. (b) Same as Figure 2a but for 16 April 2013. The upward pointing arrows depict the points where velocity estimation is performed.

for the zonal velocity to decrease with time during the course of the night. It appears that scintillation patch observed between 20:00 LT and 21:00 LT at Tirunelveli, either did not evolve or, evolved with very less intensity over Trivandrum. No further attention is paid to this point as the aim here is to estimate irregularity zonal velocity by looking in to the patch movement and since this exceptional case does not affect the present results. Figure 2b depicts the evolution of scintillation patches on 16 April 2013. Four distinct patches were observed between 20:00 LT and 02:00 LT (26:00 h). Once again, the decreasing trend of the velocity with time during the night could be clearly seen even on this day. Similar picture emerged on other days as well. Generalizing the results based on the campaign days, the velocities corresponding to all the days are plotted together in Figure 3. It can be seen that a total of 20 points from 6 days of observations have been obtained. Out of the remaining 2 days, on 1 day, scintillation had been very weak, and on another day, in spite of reasonably strong scintillations, there were no clear identifiable features for working out the time delay. It can be

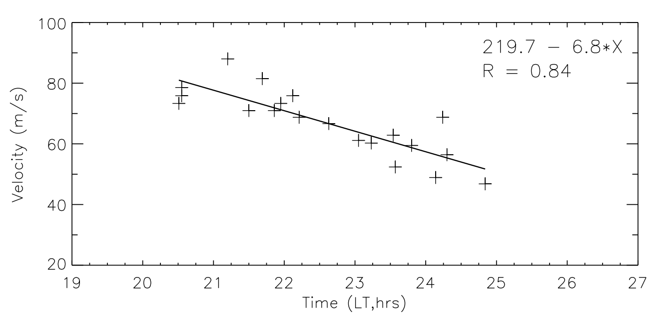

Figure 3. The velocities corresponding to all the campaign days at different local times are depicted. The decreasing trend as shown by regression line exhibits that velocity decreases with local time during the course of the night.

seen from Figure 3 that the velocity decreases with time and the linear correlation has a negative slope with correlation coefficient of ~0.84. In general, the L band scintillation was present only during 20:00 LT to 01:00 LT (25:00 h) over Trivandrum, during this epoch, and hence, the velocity estimation outside this time window is not possible. But, once the trend is established with larger number of observations, the extrapolation of the regression line can always be performed to estimate the velocity even outside this window.

Fejer et al. [1985] had stated that the average *F* region zonal drift measured using radar interferometer technique at Jicamarca was in good agreement with that of the incoherent scatter measurements. While comparing the drifts from incoherent scatter and spaced receiver measurements, they found that the drift velocities measured using the latter is very large, particularly during solar minimum. In this context, the drift velocity values, as well as the trend, obtained during the present exercise come out in broad agreement with that of *Fejer et al*. [1991]. It is felt that the present simple technique to estimate the irregularity zonal drift is highly prospective and more realistic.

The magnitude of the drift velocity at a given time obtained in the present exercise falls within ±20 m/s of error bound values of incoherent scatter measurements. *Fejer et al*. [1991] from American longitudes had shown that, for solar fluxes $<$120 solar flux unit (sfu), the background plasma drift was ~90 m/s at ~20:00 LT, attained a peak value of ~100 m/s at ~21:00 LT, and later decreased steadily with time to ~50 m/s by 01:00 LT (25:00 h), during equinoxes. It can be seen in Figure 3 that at ~20:30 LT, the drift was ~80 m/s which decreased with time to ~50 m/s by 01:00 LT (25:00 h). The solar flux $F_{10.7}$ remained $>$70 sfu and $<$120 sfu during the campaign period. Thus, the present drift values could be taken as representative for the given season and solar epoch. The above estimates can still be improved once more data become available.

4. Assessment of the Impact of the Zonal Velocity Variation in the Forecast of the Scintillation Maps

Apart from characterizing the zonal drift velocity variations, the ultimate goal is to utilize them in the generation of scintillation maps that could be used while employing satellite-based navigation and positioning. The zonal velocity of the irregularity patches, or in other words that of the perturbation, decreased significantly during the course of the night. If the perturbation velocity is known at a given time, its travel time to adjacent longitudes can be calculated. On the arrival of the favorable phase of the perturbation over a given location, depending on the favorable background conditions, irregularities could grow. *Sridharan et al*. [2012] had made a major breakthrough by successfully forecasting the temporal evolution of scintillations over an equatorial region using GPS-TEC measurements. The few slippages in their forecast method were suggested to be due to their assumption that the zonal drift velocity of the irregularities/perturbation remained constant throughout the night. Although the method was refined by *Bagiya et al*. [2014], by the usage of actually measured zonal velocities, its time variation was not accounted for. The present case study highlights the significant differences this factor could bring about in the forecast maps. All along, we had been treating the perturbation characteristics as seen in the temporal domain, while in reality what is being considered is the manifestation of the movement of the spatial structures as seen from one location. Whenever there is any change in the velocity for the same spatial structure, it would be reflected as faster/slower variations for larger/smaller velocities. Therefore, one could take that the LT variation of the velocities is already incorporated in the temporal variation of the perturbations from any given location, and they would get reflected in the wavelet analysis too. As long as the spatial structure of the perturbation are retained throughout day and night (which is the fundamental assumption all through our study), its characteristic variation would be the same at different locations, except for the local time difference due to the longitudinal separation and the perturbation velocity corresponding to that local time. We consider below two cases: (i) with uniform zonal velocity and (ii) with varying zonal velocity, and forecast the spatiotemporal maps of scintillations. The outcome is compared with actual observation of scintillations, at any location, at the corresponding local time in both the cases.

Figure 4a depicts the map with uniform velocity of 80 ms^{-1}, corresponding to 15 April 2013, when both the receivers (Trivandrum and Tirunelveli) were operated simultaneously. The shaded area with time is the duration when one could expect scintillations in that particular longitude region as per the forecast mechanism proposed by *Sridharan et al*. [2014]. The scintillation data from different locations like

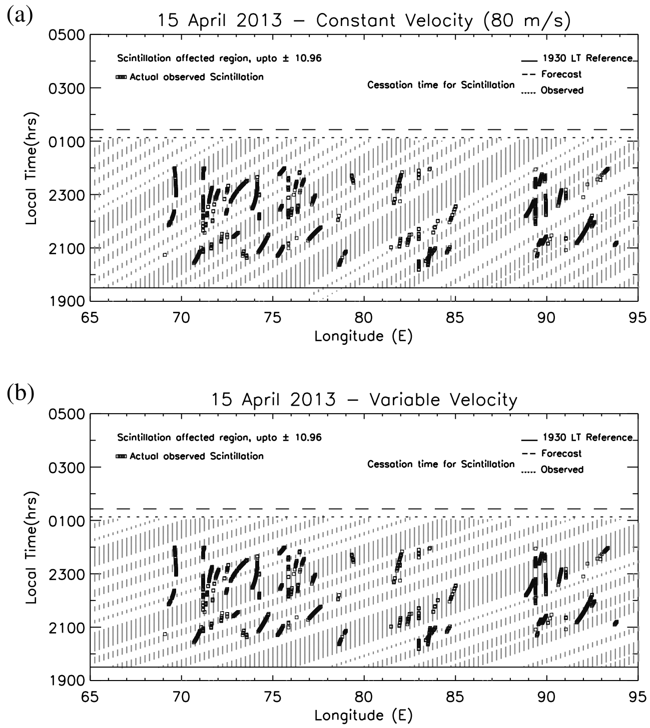

Figure 4. The spatiotemporal occurrence pattern of scintillation generated with uniform velocity of 80 ms^{-1} for 15 April 2013. The shaded area with time is the duration when one could expect scintillations in that particular longitude region. The square symbols represent the actual observed scintillation from different locations like Agati (10.83°N, 72.2°E), Trivandrum (8.5°N, 76.9°E), Visakhapatnam (17.69°N, 83.22°E), and Port Blair (11.61°N, 92.77°E).

Agati (10.83°N, 72.2°E), Trivandrum (8.5°N, 76.9°E), Visakhapatnam (17.69°N, 83.22°E), and Port Blair (11.61°N, 92.77°E) are used to cross check the validity of the forecast. The estimation of the latitude coverage along with cessation time of the scintillations have been arrived at based on the basic ionospheric parameters at 19:30 h and have been dealt in detail by *Bagiya et al.* [2013] and *Sridharan et al.* [2014]. Although the forecast attempt with uniform zonal velocity of the perturbations has been reasonably successful, as mentioned earlier, the few deviations from the forecast and the possible role of the temporal variation of the zonal velocity of the perturbation in causing them are emphasized below. Figure 4b represents the map for the same day after duly accounting for the local time variation of the zonal velocity as per the linear fit given in Figure 3.

It could be seen that the series of time bands now show a slight curvature with time and the overall distance travelled by a particular perturbation feature has changed significantly during a time span of 6 h. This figure can be understood in the following way. The fluctuating components of the perturbation over any location with time could be construed as a train of perturbations that would move eastward with a velocity corresponding to that particular local time. The negative phase of the perturbation is depicted by the shaded region. As the zonal velocity of the perturbation train would either take more or less time to cover the same longitudinal distance depending on the velocity had been larger/smaller. The perturbation train has to be shifted in time to account for this time difference before being depicted as a space versus LT map. Attention is drawn to the overall better agreement in the forecast in Figure 4b as compared to the case where the velocity had been taken as uniform (Figure 4a). It could be seen that the bands representing the time duration itself had got drastically changed, the moment the temporal variation of the velocity is taken in to account. Specifically, if one looks at the scintillation patches in the longitude zone of 80° to 95° and compares the two maps, better matching of scintillation patches becomes evident in the latter case. One should keep in mind that even with the constant velocity, there had been a fairly good agreement between the forecast and the actual occurrence and the incorporation of the temporal variation of the velocity in the forecast scheme refines the earlier forecast, and to that extent, it vindicates the earlier suggestion that the zonal velocity variation is an important factor that needs to be characterized and incorporated in any accurate forecast mechanism. As it stands, the present forecast scheme would be limited only by the deviations (i) in the forecast perturbations from the expectations and (ii) in the expected velocity variations during the course of a night. More detailed studies on the characterization of, the zonal velocity of the perturbations, the stipulated background conditions and their variabilities with seasons and solar activity are underway so as to evolve a robust forecasting method that could be used in practical applications like satellite-based navigation.

5. Conclusions

Estimation of the irregularity zonal drift velocity, using scintillation patches as a tracer, has been described using the geostationary satellite beacons at L1 band, which could be treated as representative of the moderate solar activity (70 sfu < $F_{10.7}$ < 120 sfu) levels. The zonal drift velocity is observed to decrease with local time consistent with the earlier incoherent scatter radar measurements from American longitudes for similar solar flux values. With the variable drift values, the spatiotemporal forecast of L band scintillation have become more realistic and is emerging as one of the important tools for satellite-based navigation. Although the current work deals only with the occurrence of scintillation and does not address to the actual strength of the same, further studies are on to bring in the intensity of scintillations also in the forecasting system with an aim to provide answers to the fundamental questions like “when,” “where” (spatial extent), “how long” (duration), and with “what intensity” the scintillations are likely to occur.

Acknowledgments

This work is supported by Department of Science and Technology, Government of India. The data are collected under the campaign conducted as a part of the CSIR-supported research and executed in collaboration with Space Physics Laboratory, VSSC, Trivandrum. R.S. duly acknowledges the National Academy of Sciences Allahabad for the senior scientist position and director PRL for hosting the position in PRL. L.J. acknowledges the support of NASI through his RA fellowship. S.S. duly acknowledges the support of the Airport Authority of India. The study is carried out under the national umbrella of CAWSES-INDIA program supported by ISRO/Department of Space, Government of India.

Alan Rodger thanks the reviewers for their assistance in evaluating this paper.

References

Abdu, M. A., I. J. Kantor, I. S. Batista, and E. R. de Paula (1985), East–west plasma bubble irregularity motion determined from spaced VHF polarimeters: Implications on velocity shear in the zonal *F* region bulk plasma motion, *Radio Sci.*, *20*(1), 111–122, doi:10.1029/RS020i001p00111.

Bagiya, M. S., and R. Sridharan (2011), Evolutionary phases of equatorial spread *F* including L band scintillations and plumes in the context of GPS total electron content variability: A case study, *J. Geophys. Res.*, *116*, A10304, doi:10.1029/2011JA016893.

Bagiya, M. S., R. Sridharan, and S. Sunda (2013), Pre-assessment of the “strength” and “latitudinal extent” of L band scintillation: A case study, *J. Geophys. Res. Space Physics*, *118*, 488–495, doi:10.1029/2012JA017989.

Bagiya, M. S., R. Sridharan, S. Sunda, L. Jose, T. K. Pant, and R. Choudhary (2014), Critical assessment of the forecasting capability of L band scintillation over the magnetic equatorial region—Campaign results, *J. Atmos. Sol. Terr. Phys.*, *110–111*, 15–22.

Basu, S., J. P. McClure, S. Basu, W. B. Hanson, and J. Aarons (1980), Coordinated study of equatorial scintillation and in situ and radar observations of nighttime *F* region irregularities, *J. Geophys. Res.*, *85*, 5119, doi:10.1029/JA085iA10p05119.

Bhattacharyya, A., S. Basu, K. M. Groves, C. E. Valladares, and R. E. Sheehan (2001), Dynamics of equatorial *F* region irregularities from spaced receiver scintillation observations, *Geophys. Res. Lett.*, *28*, 119–122, doi:10.1029/2000GL012288.

Chandra, H., R. K. Misra, M. R. Deshpande, and R. G. Rastogi (1970), Ionospheric irregularities and their drifts at Thumba during 1964–1968, *Indian J. Pure Appl. Phys.*, *8*, 548.

de Paula, E. R., et al. (2002), Ionospheric irregularity zonal velocities over Cachoeira Paulista, *J. Atmos. Sol. Terr. Phys.*, *64*, 1511–1516.

England, S. L., and T. J. Immel (2012), An empirical model of the drift velocity of equatorial plasma depletions, *J. Geophys. Res.*, *117*, A12308, doi:10.1029/2012JA018091.

Fejer, B. G., E. Kudeki, and D. T. Farley (1985), Equatorial *F* region zonal plasma drifts, *J. Geophys. Res.*, *90*, 12,249–12,255, doi:10.1029/JA090iA12p12249.

Fejer, B. G., E. R. de Paula, S. A. Gonzalez, and R. F. Woodman (1991), Average vertical and zonal *F*-region plasma drifts over Jicamarca, *J. Geophys. Res.*, *96*, 13,901–13,906, doi:10.1029/91JA01171.

Fejer, B. G., J. R. Souza, A. S. Santos, and A. E. C. Pereira (2005), Climatology of *F*-region zonal plasma drifts over Jicamarca, *J. Geophys. Res.*, *110*, A12310, doi:10.1029/2005JA011324.

Immel, T. J., H. U. Frey, S. B. Mende, and E. Sagawa (2004), Global observations of the zonal drift speed of equatorial ionospheric plasma bubbles, *Ann. Geophys.*, *22*, 3099–3107, doi:10.5194/angeo-22-3099-2004.

Kil, H., P. M. Kintner, E. R. de Paula, and I. J. Kantor (2000), Global Positioning System measurements of the ionospheric apparent velocity at Cachoeira Paulista in Brazil, *J. Geophys. Res.*, *105*(A3), 5317–5327, doi:10.1029/1999JA000244.

Kil, H., P. M. Kintner, E. R. de Paula, and I. J. Kantor (2002), Latitudinal variations of scintillation activity and zonal plasma drifts in South America, *Radio Sci.*, *37*(1), 6-1–6-7, doi:10.1029/2001RS002468.

Kudeki, E., B. G. Fejer, D. T. Farley, and H. M. Ierkic (1981), Interferometer studies of equatorial *F* region irregularities and drifts, *Geophys. Res. Lett.*, *8*, 377–380, doi:10.1029/GL008i004p00377.

Ledvina, B. M., P. M. Kintner, and E. R. de Paula (2004), Understanding spaced receiver zonal velocity estimation, *J. Geophys. Res.*, *109*, A10306, doi:10.1029/2004JA010489.

Martinis, C., J. V. Eccles, J. Baumgardner, J. Manzano, and M. Mendillo (2003), Latitude dependence of zonal plasma drifts obtained from dual-site airglow observations, *J. Geophys. Res.*, *108*(A3), 1129, doi:10.1029/2002JA009462.

Misra, R. K. (1973), Fading characteristics and drift and anisotropy parameters of the ground diffraction pattern of the radio waves reflected from the ionosphere during spread-*F* conditions, *J. Geophys. Res.*, *78*, 5703–5709, doi:10.1029/JA078i025p05703.

Muella, M. T. A. H., E. R. de Paula, I. J. Kantor, L. F. C. Rezende, and P. F. Smorigo (2009), Occurrence and zonal drifts of small-scale ionospheric irregularities over an equatorial station during solar maximum—Magnetic quiet and disturbed conditions, *Adv. Space Res.*, *43*, 1957–1973.

Nade, D. P., A. K. Sharma, S. S. Nikte, P. T. Patil, R. N. Ghodpage, M. V. Rokade, S. Gurubaran, A. Taori, and Y. Sahai (2013), Zonal velocity of the equatorial plasma bubbles over Kolhapur, India, *Ann. Geophys.*, *31*, 2077–2084.

Oliver, W. L., Y. Otsuka, M. Sato, T. Takami, and S. Fukao (1997), A climatology of *F* region gravity wave propagation over the middle and upper atmosphere radar, *J. Geophys. Res.*, *102*, 14,499–14,512, doi:10.1029/97JA00491.

Ossakow, S., and P. K. Chaturvedi (1978), Morphological studies of rising equatorial spread *F* bubbles, *J. Geophys. Res.*, *83*, 2085–2090, doi:10.1029/JA083iA05p02085.

Otsuka, Y., K. Shiokawa, and T. Ogawa (2006), Equatorial ionospheric scintillations and zonal irregularity drifts observed with closely-spaced GPS receivers in Indonesia, *J. Meteorol. Soc. Jpn.*, *84*, 343–351.

Rastogi, R. G., H. Chandra, and R. K. Misra (1972), Features of the ionospheric drifts over the magnetic equator, *Space Res.*, *12*, 984.

Sridharan, R., M. S. Bagiya, and S. Sunda (2012), A novel method based on GPS TEC to forecast L band scintillations over the equatorial region through a case study, *J. Atmos. Sol. Terr. Phys.*, *80*, 230–238.

Sridharan, R., M. S. Bagiya, S. Sunda, R. Choudhary, T. K. Pant, and L. Jose (2014), First results on forecasting the spatial occurrence pattern of L band scintillation and its temporal evolution, *J. Atmos. Sol. Terr. Phys.*, *119*, 53–62.

Tsunoda, R. T. (1981), Time evolution and dynamics of equatorial backscatter plumes, 1, Growth phase, *J. Geophys. Res.*, *86*, 139–149, doi:10.1029/JA086iA01p00139.

Yeh, K. C., and C. H. Liu (1982), Radio wave scintillations in the ionosphere, *Proc. IEEE*, *70*, 324–360.